Development of an internal air cooling sprayed oil injection technique for the energy saving in sliding vane rotary compressors through theoretical and experimental methodologies

Giuseppe Bianchi[a,*], Roberto Cipollone[a], Stefano Murgia[b], Giulio Contaldi[b]

[a] *Department of Industrial and Information Engineering and Economics, University of L'Aquila, Via Giovanni Gronchi 18, 67100 L'Aquila, Italy*
[b] *Ing. Enea Mattei S.p.A., Strada Padana Superiore 307, 20090 Vimodrone, Italy*

Abstract

The present work highlights the energy saving potential of the lubricant fluid supplied in Sliding Vane Rotary air Compressors. A Lagrangian theoretical model of a sprayed oil injection technology assessed the cooling effect of the lubricant due to the high surface to volume ratio of the oil droplets and predicted a reduction of the indicated power. The model validation was carried out through a test campaign on a mid-size sliding vane compressor equipped with a series of pressure swirl atomizers. The oil injections took place along the axial length of the compressor. The reconstruction of the indicator diagram and the direct measurement of the mechanical power revealed a reduction of the energy consumption close to 7 % using an injection pressure of 20 bar. A parametric analysis on the injection pressure and temperature and on the cone spray angle was eventually carried out to identify an optimal set of operative injection parameters.

Keywords: sliding vane rotary compressor, compressed air systems, oil injection, pressure swirl nozzle, indicator diagram, piezoelectric pressure transducer

*Corresponding author

NOMENCLATURE

γ	half of cone spray angle	$[deg]$	Nu	Nusselt number	$[-]$
θ	angular coordinate	$[deg]$	Pr	Prandtl number	$[-]$
λ	latent heat of vaporization	$[J]$	$\dot{Q}$	thermal power	$[W]$
μ	dynamic viscosity	$[Pa\,s]$	R	radius	$[m]$
ρ	density	$[kg/m^3]$	Re	Reynolds number	$[-]$
σ	surface tension	$[N/m]$	Sc	Schmidt number	$[-]$
ω	revolution speed	$[RPM]$	Sh	Sherwood number	$[-]$
c_p	specific heat at constant pressure	$[J/kg/K]$	T	temperature	$[K]$
d	droplet diameter	$[m]$	V	velocity	$[m/s]$
k	thermal conductivity	$[W/m/K]$	**Subscrips and superscripts**		
m	mass	$[kg]$	a	air	
$\dot{m}$	mass flow rate	$[kg/s]$	cor	Coriolis	
n	number	$[-]$	d	droplet	
p	pressure	$[Pa]$	ev	evaporation	
B_M	Spalding mass transfer number	$[-]$	inj	injection/injector	
B_T	Spalding heat transfer number	$[-]$	m	air-oil vapors mixture	
C_d	drag coefficient	$[-]$	o	oil	
D	molecular diffusivity	$[m^2/s]$	or	orifice	
F	force	$[N]$	$*$	corrected	

1. INTRODUCTION

Compressed air accounts for a mean 10 % of the global industrial electric energy consumptions (Radgen, 2001) and this share may reach 20 % if commercial and residential needs are included (portable tools, air pumps, pneumatic heating, ventilation, air conditioning, etc) (US Department of Energy, 2003). In order to accomplish global energetic and environmental commitments, energy saving is nowadays recognized as the main action that needs to be put into action. Within this framework, in Compressed Air Systems (CAS) lots of saving measures have been employing with efforts upstream and downstream of the compressed air production: pipeline leakages reduction, CAS design, adjustable speed drives, optimization of the end use devices, frictional losses, etc. As concerns the compressor technology, the saving potential was estimated to be around 10-20 % (740 TWh in 2012) (Cipollone and Vittorini, 2014, Vittorini et al., in press). In industrial applications, rotary volumetric machines are the most widespread technology in the range 7-12 bar and flow rates less than 1000 m^3/min with an electrical power from a few kW to several hundred kW. Among them, Sliding Vane Rotary Compressors (SVRC) represent only few points percent of the overall market. However, they have some intrinsic features which state an unforeseen potential. Indeed, a recent study on the energy reduction perspectives in positive displacement machines stated that SVRCs behave more efficiently than screw compressors if on\off load conditions were taken into account while estimating the energy consumptions (Cipollone, 2014). In order to additionally increase the premium performance of SVRCs, a thermodynamic improvement was highlighted approaching the current adiabatic transformation towards an isothermal one by means of a sprayed oil injection technology that preliminary demonstrated its ability to internally cool the air during the compression phase (Cipollone et al., 2012, 2013, 2014).

The performance enhancement through a sprayed oil injection technology has been assessed almost exclusively on screw compressors. Mathematical models on heat transfer between oil droplets and air have been set up (Seshaiah et al., 2007, Stosic et al., 1988) as well as experimental activities on the sole atomizers (Paepe et al., 2005) or the whole compressor test rig have been carried out (Stosic et al., 1992, Fujiwara and Osada, 1995), even using different working fluids (Seshaiah et al., 2010). Among them, a reduction on the energy consumptions from 2.8 % to 7.4 % was assessed (Stosic et al., 1992). The roles of the main injection parameters have been investigated: injection pressure and temperature, oil flow rate, orifice diameter (Paepe et al., 2005), injectors positioning (Ferreira et al., 2006), etc.

In the current work, the Authors pursued the investigation of the effects due to spraying the oil in sliding vane compressors presenting a comprehensive theoretical model for the axial injection. The model was further validated through tests on a mid-size SVRC equipped with pressure swirl nozzles. A series of piezoelectric pressure transducers allowed to assess an overall matching between the simulations and the experimental indicator (pressure-Volume) diagram. A parametric analysis on the main injection operating parameters eventually addressed further improvements to the innovative injection technology.

2. AXIAL OIL INJECTION MODELING

The oil sprayed injection was modeled following a lumped parameter approach for the thermodynamics of the compressor cells, while a Lagrangian one was adopted to track the oil particles and their interactions with air. The injectors were located on a side cover of the machine such that the oil droplets sprayed propagated along the axial direction of the compressor. The model aimed at understanding the interactions between oil sprays and compressing air in order to identify the optimal set of injection parameters to address the experimental activity. To ease the computations without losing the physics behind the model, some assumptions were made: among them, a two dimensional approach was used to detect the spray evolution within the rotating cells. Hence, for each injector at a given angular position, the frame of reference chosen for the study was the radial-axial plane. Furthermore, the way of subdividing the spray in droplets packages having different injection angles also led to neglect secondary phenomena like droplets coalescence. The overall structure of the model is schematized in Figure 1: after the spray formation, the 2D conservation equations applied to each droplet package provide input data (in terms of overall heat exchanged between air and oil and mass of oil vapors) to calculate the thermodynamic state of the compressor cell with a lumped parameter (0D) approach. The mathematical model was implemented in the Mathworks Matlab® environment and resulted in a simulation platform whose validation and capabilities are discussed in the following sections.

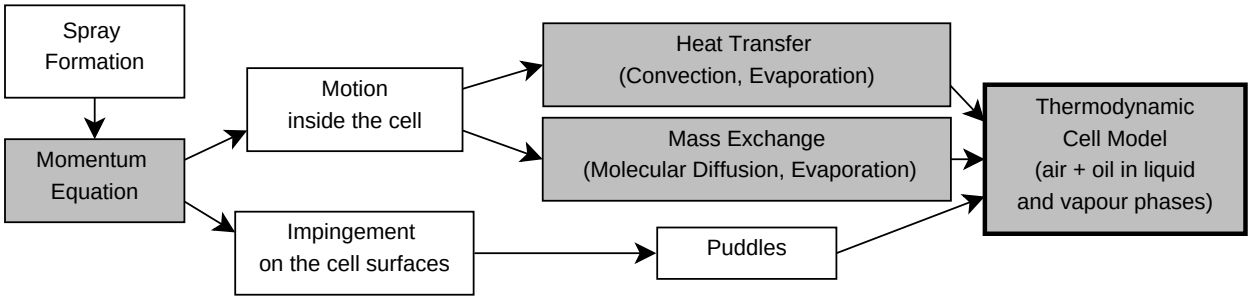

Figure 1: 1. Conservation equations applied to the oil droplets after the spray breakup and interactions with the thermodynamics of the compressor cell

2.1. Spray formation

Using pressure-swirl atomizers and proper injection pressures, the oil jets breakup in a multitude of droplets having different sizes (Valenti et al., 2013). Experiments on the same nozzles found that the droplet size distribution resembles the Rosin Rammler function (Laryea and No, 2004) with a Sauter Mean Diameter (SMD) estimated according to the empirical correlation in Equation 1 (Liu, 1999).

$$SMD = 4.52\left(\frac{\sigma_o \mu_o^2}{\rho_a\,\Delta p}\right)^{0.25}\left[2.7\left(\frac{d_{or}\,\dot{m}_o\,\mu_o}{\rho_o\,\Delta p}\right)\cos\gamma\right]^{0.25} + 0.39\left(\frac{\rho_o \mu_o}{\rho_a\,\Delta p}\right)^{0.25}\left[2.7\left(\frac{d_{or}\,\dot{m}_o\,\mu_o}{\rho_o\,\Delta p}\right)\cos\gamma\right]^{0.75} \quad (1)$$

where γ is the half the cone spray angle, d_{or} the orifice diameter and Δp the pressure difference across the nozzle. The latter parameter not only depends on the injection pressure but also on the injectors positioning: as they move towards the end of the compression phase, the air pressure increases and leads to smaller Δp, thus greater SMD.

The thermo-physical properties of the lubricant were evaluated using semi-empirical correlations (Conde, 1996, Mermond et al., 1999, Lottin et al., 2003) tuned with experimental data from the oil manufacturer: specific gravity 0.95, kinematic viscosity 99 cSt at $40°C$ and 10.2 cSt at $100°C$.

With reference to the same rotating cell, for each atomizer the injection starts when the first blade with respect to the direction of rotation encounters the injector and ends when the second blade leaves it. Therefore, the single injection duration depends on the number of cells and on the angular velocity. If multiple injectors are installed along the angular displacement of the compression phase, the duration is imposed by the overlapping of the first and last injectors, as reported in Equation 2

$$\Delta t_{inj}: \qquad \frac{2\pi}{n_{cell}\omega} \quad (n_{inj}=1) \qquad \frac{1}{\omega}\left[\theta_{inj,last} + \frac{2\pi}{n_{cell}} - \theta_{inj,1st}\right] \quad (n_{inj}>1) \quad (2)$$

The oil mass supplied was equally distributed in N_t sub-injections sequentially spaced in time. In each sub-injection, the droplet size distribution was further discretized in N_d parcels that grouped diameter classes close to each other. Each parcel had a different initial direction, chosen according to a Gaussian density distribution. The assumed cone angle was that containing a $\pm 3\sigma$ amplitude on each side of the spray center line to simulate the spray density variation along transverse direction. The initial velocity of all particles was set equal to the jet velocity (Laryea and No, 2004, Chen et al., 1993) while the initial temperature of all the droplets was equal to the one of the oil downstream the cooler (available from experimental data).

2.2. Interaction between Oil droplets and Air

After the breakup, each of the N_d parcels of oil droplets travels inside the compressor cells whose volume variation influences the thermodynamic properties of the medium in which the spray propagates. In order to study how oil droplets interacted with the compression process, a coupling of the conservation equations written in a Lagrangian form was adopted according to the scheme in Figure 1. The time in which an effective heat transfer between the oil and the air occurs is equal to the residence time of the oil as droplets i.e. from the spray breakup until the impingement on the metallic surfaces of the cell. Afterwards, the liquid oil film that builds up on the vane surfaces does not succeed to affect the compression anymore, as it happens in the current injection technology (liquid jets).

In order to track droplets trajectories, the momentum equation was applied in the radial-axial frame of reference relative to each injector (R,z,$\theta_{inj,i}$), as shown in Figure 2. In the most general approach, a droplet that moves in air is subjected to aerodynamic forces (drag and shear lift), inertial and fictitious forces (virtual mass, Bassett history, centrifugal, Coriolis), volume forces (gravity and buoyancy) and pressure forces (Aggarwal and Peng, 1995). With reference to previous studies, most of these contributions become negligible when compared with drag, centrifugal and Coriolis forces (Cipollone et al., 2012, C.N. Brown, 1991). Moreover, since droplets propagate along the R-z plane, the Coriolis force doesn't lie on the frame of reference but its perpendicular to it. However, its magnitude depends on the angle between droplet velocity and angular velocity vector that cannot exceed the half of the cone spray angle. Due to the tightness of the gap between stator and rotor, for axial injections nozzles with narrow cone spray angles should be used to prevent that most of the spray would suddenly impinge on the cell surfaces. In accordance with this assumption, the effects of the Coriolis force on the droplets trajectories were neglected and the final expression for the momentum equation became the one reported in Equation 3, whereas the droplet evaporation was taken into account in the term $\overrightarrow{V_d}\, dm_d/dt$.

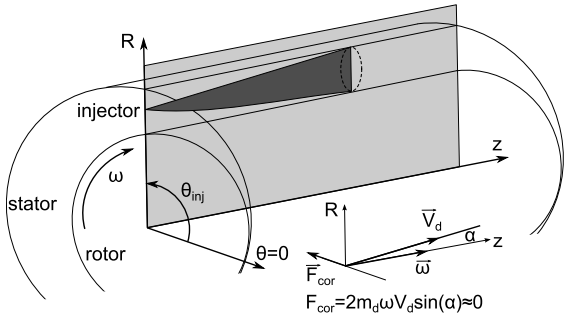

Figure 2: Radial axial reference plane for the 2D analysis of the droplets evolution within the compressor vanes

$$\overrightarrow{V_d}\frac{dm_d}{dt} + m_d\frac{d(\overrightarrow{V_d})}{dt} = \overrightarrow{F}_{drag} + \overrightarrow{F}_{centrifugal} \tag{3}$$
$$\overrightarrow{F}_{drag} = -\frac{\pi}{8}\, C_d\, d_d^2 \rho_a (\overrightarrow{V_d})^2$$
$$\overrightarrow{F}_{centrifugal} = m_d\, \omega^2 \overrightarrow{R}$$

As long as the droplets travel within the compressor cells, they exchange mass and heat with the air. Moreover, depending on the oil saturation pressure at the cell temperature, evaporation or even condensation might occur. From an energetic point of view, the first phase change enhances the air cooling but, at the same time, provides oil vapors that need to be compressed as the air does so leading to an increase of the useful specific work per unit air. On the other hand, if saturation conditions were established inside the cell,

oil vapors would condensate releasing the latent heat to the air with an increase of the compression work as well. Therefore, the target to reach with the sprayed injection technology is to maximize the heat transfer between oil and air without reaching any oil phase change. The overall heat transfer between oil and air was modeled according to the energy equation for the droplet (Equation 4).

$$\frac{d}{dt}\Big[m_d\, c_{p_d}(T_d - T_m)\Big] = \dot{Q}_{a-d} \tag{4}$$

where the subscript m refers to the thermodynamic properties of the mixture between air and oil vapors inside the compressor cell whose calculations were performed according to the one-third rule (Abramzon and Sazhin, 2006).

Even if the oil temperature does not reach the boiling conditions, some oil mass may evaporate by molecular diffusion between drop surface and air. According to the Spalding low pressure film evaporation theory, which assumes that heat and mass exchanges between the droplet surface and the gas flow can be modeled as the ones occurring within the spherical gas films of constant thickness (Abramzon and Sazhin, 2006), the heat transfer between air and droplet as well as the evaporating mass flow-rate can be calculated solving the energy and mass balance for the region around the droplet (Han et al., 1997). This leads to Equations 5 and 6 respectively:

$$\dot{Q}_{a-d} = \pi\, d_d\, k_m\, Nu^*\, (T_a - T_d) \tag{5}$$

and

$$\dot{m}_{ev} = \pi\, d_d\, D_m\, \rho_m\, Sh^*\, \ln(1 + B_M) \tag{6}$$

On the other hand, at boiling conditions the calculation of the oil mass flow rate which vaporizes $\dot{m}_{ev}$ involves the latent heat of vaporization λ according to Equation 7.

$$\dot{m}_{ev} = \frac{\dot{Q}_{a-d}}{\lambda} \tag{7}$$

The corrected Nusselt (Nu^*) and Sherwood (Sh^*) numbers, whose correlations are reported in Equation 8, depend on the Schmidt number (Abramzon and Sazhin, 2006) and the heat (B_T) and mass (B_M) transfer numbers formulated by (Spalding, 1953).

$$Nu^* = \frac{2 + B_T\,(0.552\, Re^{1/2}\, Pr^{1/3})}{(1 + B_T)^{0.7} \ln(1 + B_T)} \tag{8a}$$

$$Sh^* = \frac{2 + B_M\,(0.552\, Re^{1/2}\, Sc^{1/3})}{(1 + B_M)^{0.7} \ln(1 + B_M)} \tag{8b}$$

The continuity equation for the oil eventually takes into account oil phase changes that might occur and the liquid film formation on the metallic surfaces of the cell. Assuming that if condensation occurred that mass would feed the oil film, for a given injector Equation 9 applies.

$$\dot{m}_{inj} = \dot{m}_d + \dot{m}_{film} + \dot{m}_{ev} \tag{9}$$

In the present application, being the volatility as well as mass diffusivity of the oil used very low and the dimensions of the droplets atomized not enough small to vaporize, the latter contribution assumes a secondary influence. Hence, the overall heat transfer is driven by the forced convection between oil droplets and air.

2.3. Cell thermodynamics

At the moment, oil injection in sliding vane compressors, as well as in other volumetric machines, accomplishes lubrication and sealing purposes. This latter feature prevents flow leakages between adjacent cells, and through the side covers of the machine. Assuming a perfect sealing, the cell behaves as a closed system with respect to the air that is trapped at the suction end, compressed and eventually discharged. As concerns the gaseous fluids in the vane, the only mass transfers that may occur are the droplets evaporation (positive) or their condensation (negative). Hence, the working fluid inside the cell is a mixture of air and oil vapors that are assumed to behave as a mixture of ideal gases. Furthermore, the cell thermodynamics was investigated with a lumped parameter approach that led to uniform thermodynamic properties (pressure, temperature, composition etc.). The cell pressure was calculated solving the first derivative of the equation of state. On the other hand, the temperature evolution inside the cell was evaluated according to the first law of the thermodynamics neglecting secondary heat transfer phenomena as the one between air and oil film whose topology is continuously modified by the blade sliding within the rotor slots and at the contact point between the tip and the inner surface of the stator. Both quantities involve condensation flow rate and latent heat. This phase change occurs if the oil vapor mass exceeds the saturation mass at the cell temperature (Cipollone et al., 2012).

3. EXPERIMENTAL VALIDATION

The mathematical model was validated trough tests on a mid-size industrial sliding vane compressor equipped with a series of pressure-swirl nozzles whose features were recently investigated by (Valenti et al., 2013). Their visualizations showed a breakup length, i.e. the distance from the nozzle orifice that the liquid jet requires to achieve an atomized regime of droplets, around 20 mm at 2 bar and 60 $°C$. Using semi-empirical correlations, this datum allowed to estimate the orifice diameter of the nozzle in 1 mm. Additional information that became the input parameters for the model were the half of cone spray angle ($\gamma = 40°$) and the nominal flow rate ($2.0 - 2.5\, l/min$ at $\Delta p = 10\, bar$).

Figure 3 reports the test and instrumentation layouts with air, cooling water and oil paths. The compressor performances were investigated through the reconstruction of the indicator diagram of the machine

that was carried out using a set of four Kistler® 601A piezoelectric pressure transducers whose output data from the Kistler® 5064B21 charge amplifiers were sampled through a National Instruments® SCXI-1530 board at 10 kHz. Furthermore, measuring torque and revolution speed through a Kistler® 4504B1K torque meter led to an accurate estimation of the mechanical efficiency of the compressor.

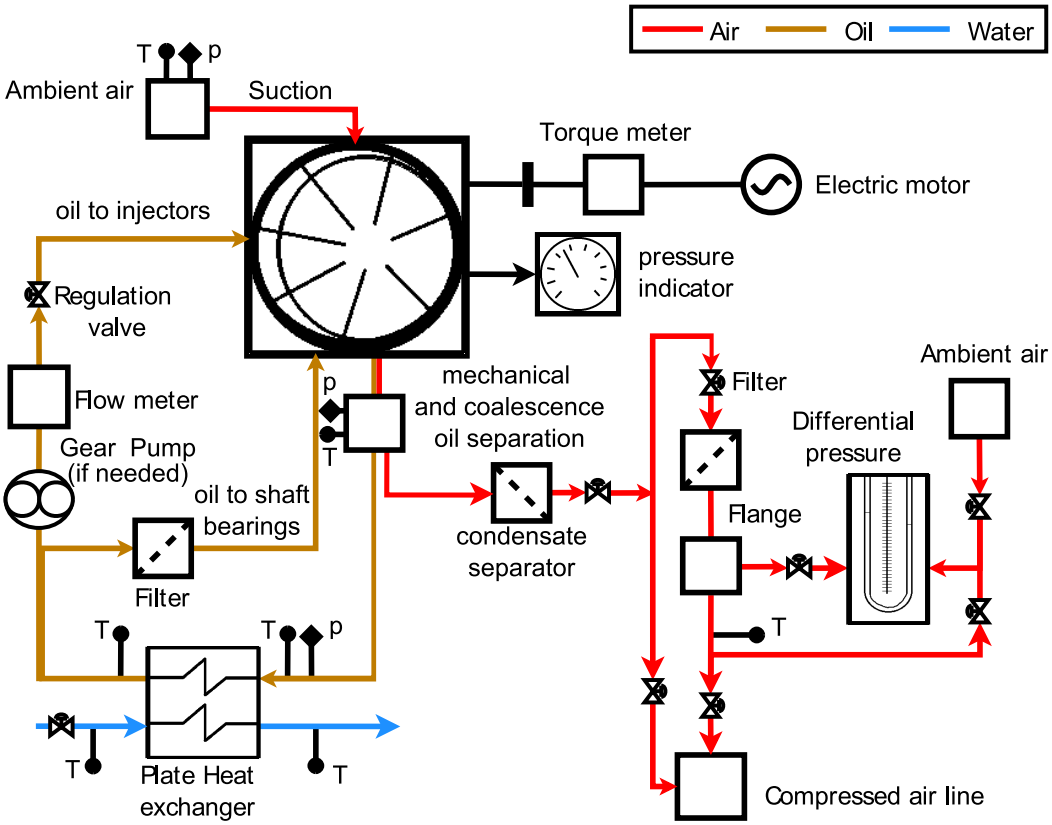

Figure 3: Layout and instrumentation of the experimental test bench along the air, oil and cooling water circuits

In the conventional injection technology, oil is supplied through calibrated holes along the axial length of the compressor thanks to the pressure difference between oil tank (whose value is close to the discharge pressure) and the cell one at the injectors location (248°). On the contrary, the spray injection technology involved a distributed positioning of the five nozzles on both the side covers of the compressor according to Figure 4 and Table 1. A picture of the compressor tested showing the injectors installation is displayed in Figure 5. The atomizers were located such that the oil temperature at the injection locations was lower than the air one. Otherwise the oil sprays would have led to a negative effect from the energetic viewpoint (air heating instead of cooling). Since air temperature increases along the compression process, the maximum temperature difference occurs at the end of it. However, these angular locations are characterized by a tight gap between stator and rotor that would have led to an almost complete impingement of the spray onto the metallic surfaces of the compressor cells. For these reasons, the injectors positioning selected is a suitable

trade-off to maximize the heat transfer between air and oil.

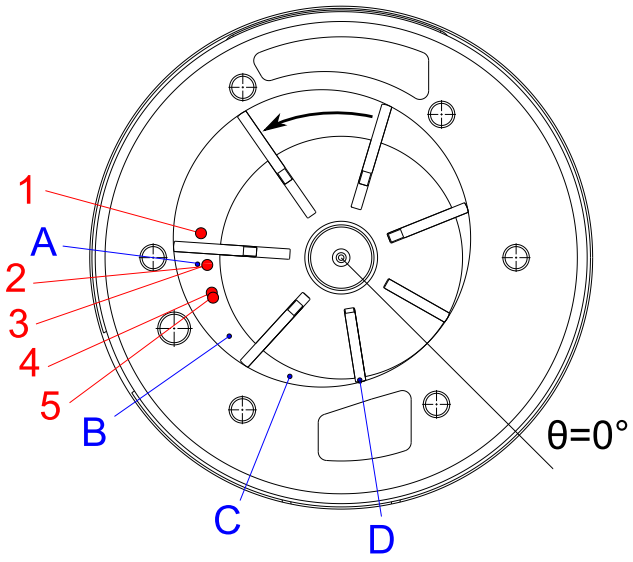

Figure 4: Cross section of the sliding vane compressor tested with injectors (numbers) and piezoelectric sensors (letters) locations

# inj	θ	# piezo	θ
1	215°	A	228°
2	228°	B	260°
3	228°	C	292°
4	240°	D	324°
5	244°		

Table 1: Injectors and piezoelectric sensors positioning

Furthermore, to boost the injection pressure, a gear pump was used to achieve finer atomizations. In both cases, downstream the compressor outlet the oil is separated from the mixture with air, recycled and cooled to be injected again. The operating conditions for the reference test case and the measurement uncertainty are listed in Table 2. In particular, the uncertainty of the mass flow measurement through the calibrated flange (ISA 1392 nozzle) was evaluated using the methodology proposed in EN ISO 5167-3 while the one associated to the reconstruction of the indicator diagram was estimated using the concept of indicated mean effective pressure proposed by (Bianchi and Cipollone, in pressa,i).

Figure 6 shows the comparison between experimental data and the compression trend calculated with the model in the pressure-volume diagram. The duration of each injection is also expressed in terms of volume ranges at the middle right of the chart. The overlapping of injection ranges led to a superposition

Figure 5: Mid-size sliding vane compressor equipped with three pressure-swirl injectors installed on an endwall plate and fed through the white colored high pressure pipes (the remaining two atomizers were installed on the opposite side cover)

Table 2: Test parameters (relative uncertainties refer to measured values)

	ω	p_{outlet}	oil flow rate	p_{inj}	T_{inj}	air mass flow rate	indicated power	shaft power
	RPM	bar_a	L/min	bar_a	$°C$	kg/s	kW	kW
oil spray	1498	8.50	31	20.20	60.0	0.070	19.4	21.4
oil jets	1500	8.50	37	7.90	67.4	0.069	20.9	23.1
Uncertainty	1	0.03	1	0.03	0.3	4%	4.3%	0.2%

of the effects associated to each injector that implied an enhanced heat transfer. The effectiveness of the innovative oil injection technique can be noticed both from experimental and theoretical viewpoints. The blue trace represents the indicator diagram at the same operating point but with the conventional injection technology (oil jets at 8 bar). As can be observed from the overlapping with the dashed line, in this case the compression phase is adiabatic. On the other hand, the black line below the adiabatic trend represents the indicator diagram affected by the heat exchange due to the oil sprays. The gap between the adiabatic and polytropic trends increases in correspondence of the overlapping of multiple injections while becomes constant after the injection end. Therefore, as the cooling effect ends, the compression becomes again

adiabatic until the discharge takes place. The complexity of the physical phenomena involved in the first part of the injection (droplets collisions and coalescence, 3D sprays) and the assumptions on which the model was developed motivate the mismatching between the experimental and calculated trends. Nevertheless, the model matches the cell pressure reached at the injection end and it is able to follow the pressure evolution in the last part of the compression phase. The difference between the areas of the indicator diagrams referred to the blue (oil jets) and black (oil sprays) curves in Figure 6 is the effect of the air cooling due to the novel injection technology. This quantity is composed of a contribution related to the closed-volume compression phase, equal to the thermal power exchanged between air and oil, and another one that occurs during the air discharge, a complex unsteady phenomenon which results from the interaction between the compressor cells and discharge volumes downstream. As can be noticed in Figure 6, the areas difference at the discharge is of secondary relevance compared to the one along the closed volume compression process. Hence, with reasonable approximation, the thermal power exchanged between and air can be considered equal to the energy benefit achieved. Although the indicated power is affected by the uncertainty due to the reconstruction of the p-V diagram, an accurate indication of the energy saving benefit achieved is provided by the difference in the mechanical power that is equal to 1.7 kW (7.3 %). This quantity is only due to the cooling effects of the oil and it is not discounted by the energy consumption of the gear pump which is present being the injection pressure higher than the line pressure.

With reference to Figure 7, the simulated droplets trajectories can be observed in the radial-axial plane for the injector #1 at 215.4°. The spray takes place downstream the breakup length of 7 mm, in agreement with the experimental trends available in literature. After that, the different parcels of droplets propagate with a direction within the nozzle cone spray angle. Depending on the magnitude and direction of the deviation, some of the particles suddenly impinge either on the rotor or on the stator wall. On the other hand, the straight propagation of the packages in the middle of the spray is mainly influenced by the centrifugal force that accelerates the droplets towards the stator. Hence, the magnitude of the deviation is proportional to the square of the revolution speed of the compressor. The drag and inertia forces also affect the droplets motion. Big droplets have a higher inertia that delays the decelerating effects of the drag and the deviation due to the centrifugal force such that they tend to travel along the whole axial length of the compressor. Conversely, the small droplets deviate quite soon.

From a heat transfer point of view, small droplets have a higher surface to volume ratio and seem to be the most suitable ones to enhance the cooling effects of the spray. On the other hand, the residence time for the heat exchange from the breakup until the impingement is short.

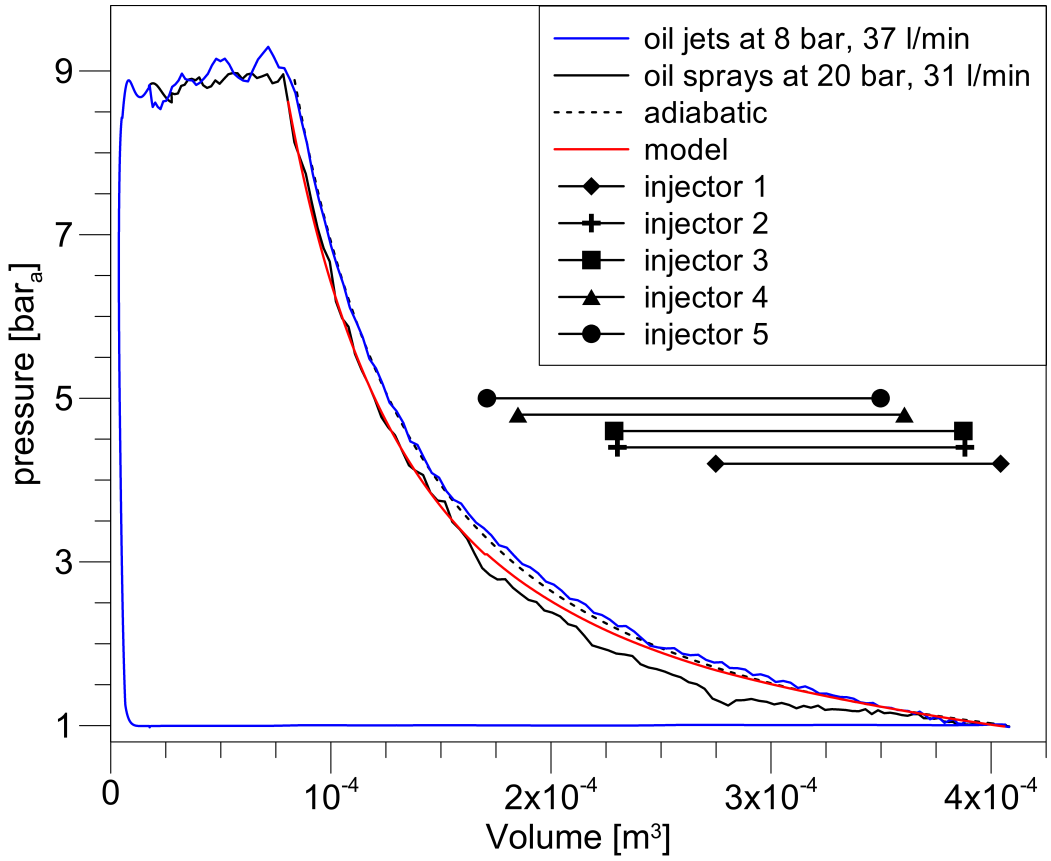

Figure 6: Comparison between the current injection technology and the sprayed one through experimental indicator diagrams and theoretical compression trends

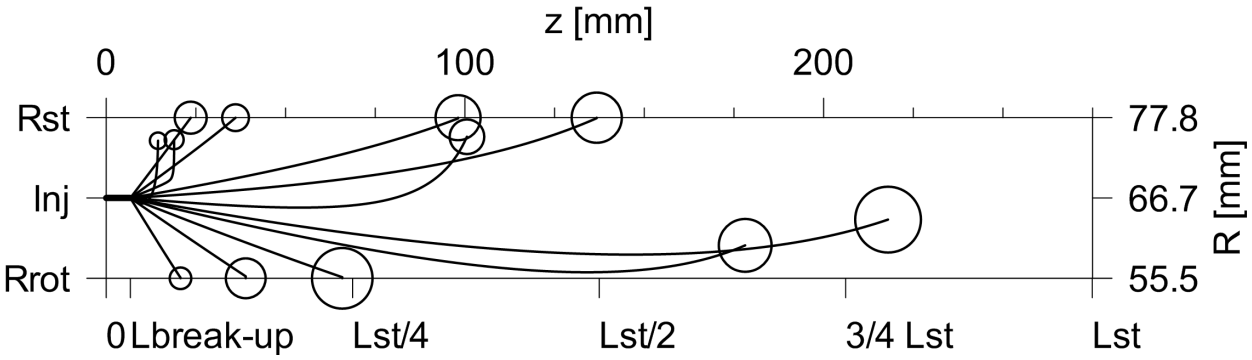

Figure 7: Spray propagation along the axial length of the compressor at $\theta = \theta_{inj,1} = 215°$ the chart is in scale while the circles are proportional to the diameter of the droplets

4. PARAMETRIC ANALYSIS

Once the simulation platform of the axial oil injection was developed and experimentally validated, a model based analysis was carried out aiming at improving the energy saving features of the oil spray jets

addressing the most relevant operating parameters for a further refining of the technique. Among them, the study presented herein focused on the oil pressure and temperature at the injection and on the cone spray angle of the nozzle. Despite the incompressibility of the oil, the first injection parameter is directly related to the energy consumption of the pressurizing device and directly affects the overall efficiency of the system (SVRC + pump). As concerns the oil temperature, its effects are imperative to keep the lubrication features within acceptable operating ranges but also for the injectors positioning: the oil must be always colder than the air at a given angular location. The cone spray angle eventually affects the amount of oil impinged on the cell surfaces without performing an effective cooling. In all the simulations, the injectors positioning and the oil rate were kept constant. As discussed in the previous section, results presented in terms of thermal power exchanged between oil and air reasonably approximate the energy saving potential achievable.

Figures 8 and 9 analyze the role that injection pressure and temperature play on a key indicator concerned to the heat exchange capabilities of the spray, namely the Sauter Mean Diameter (SMD): varying the operating conditions of the injection affects the thermo-physical properties of the oil. In particular, the dynamic viscosity decreases with temperature while the density increases with the injection pressure. Both these facts lead to a finer spray, thus a smaller SMD as reported in Figure 8. A more prominent influence of the pressure can be noticed: at 60 $^{\circ}C$, doubling the pressure from 5 to 10 bar would decrease the SMD from 183 μm to 123 μm and up to 86 μm whether the oil pressure reached 20 bar. Being the trend asymptotical, higher injection pressures do not lead to significant improvements to the SMD reduction thus to overall heat transfer, as Figure 9 shows. In order to achieve a finer spray, the injection temperature could be also increased. However, in this way the temperature difference between oil and compressing air would decrease or even reversed. On the other hand, colder oil injections would enhance the thermal power exchanged up to 30 % going from 60 $^{\circ}C$ to 30 $^{\circ}C$ at all the pressure levels simulated. Since in current machines the oil is pressurized by the compressor itself, a maximum value for the oil pressure should be fixed and set equal to the line pressure. In this way, the auxiliary pump could be avoided and the energy benefit (from the enhanced heat transfer) would become net. Feeding the injectors with oil at 10 bar, close to the usual line operating pressure, and at 70 $^{\circ}C$, the SMD would stay around 120 μm and the cooling effect in this machine would be close to 1 kW.

Figure 10 reports the non-dimensional rate of growth of the liquid film due to the impingement of the droplets onto the metallic surfaces of the compressor vanes. The analysis was carried out varying the nozzle cone spray angle (2γ) at the same oil rate of the test conditions. In order to keep the same deviation induced by the centrifugal effects, the revolution speed was also kept constant. At all the cone apertures, after the breakup droplets propagate within the cone spray whose cross section increases along the axial direction (z) until the outer particles reach the stator and rotor surfaces, as presented in Figure 7. Wide cone angles lead to steeper and bigger film formations. Although the puddles build up almost immediately, the film establishment can be delayed narrowing the spray. The steep growth of the film is damped by the

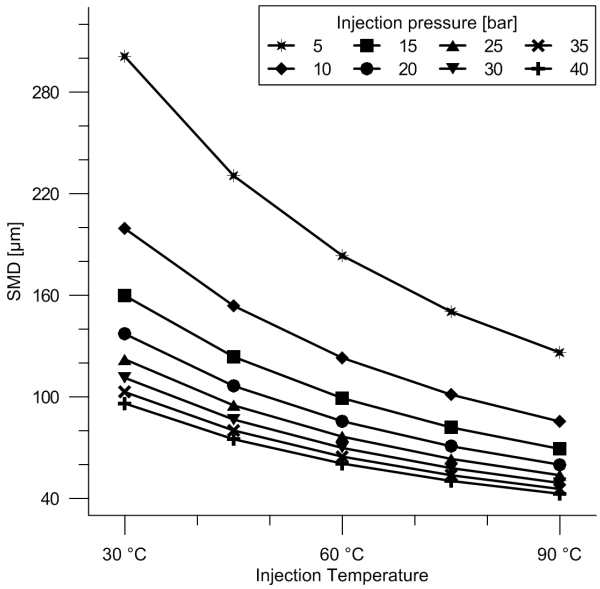

Figure 8: Effects of the oil pressure and temperature at the injection on the spray SMD

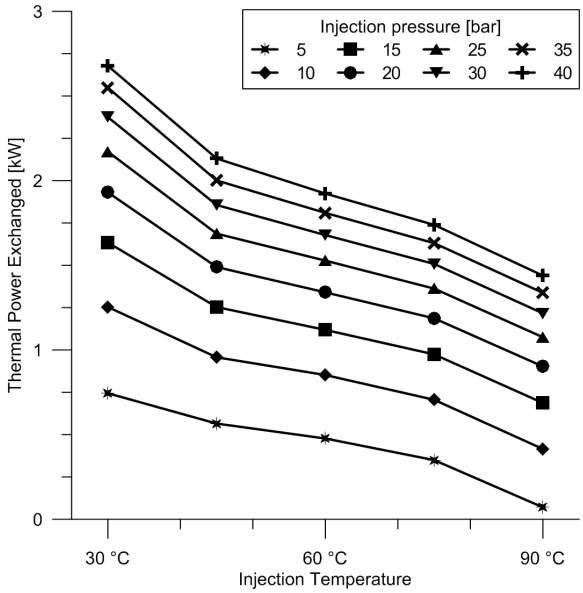

Figure 9: Effects of the oil pressure and temperature at the injection on the thermal power exchanged

oil supplied through injectors #2 and #3. From this point on, injections balance impingements and the rate of growth tends to be stabilized to percentages proportional to γ.

The effects of the cone spray angle on the overall thermal power exchanged are twofold: using nozzles with wide cone apertures produce smaller droplets (SMD decreases according to Equation 1) that tend to impinge more suddenly on the metallic surfaces of the compressor cells. However, the remaining ones, which succeed to travel inside the compressor cell, have a greater heat exchange capability due to the high surface

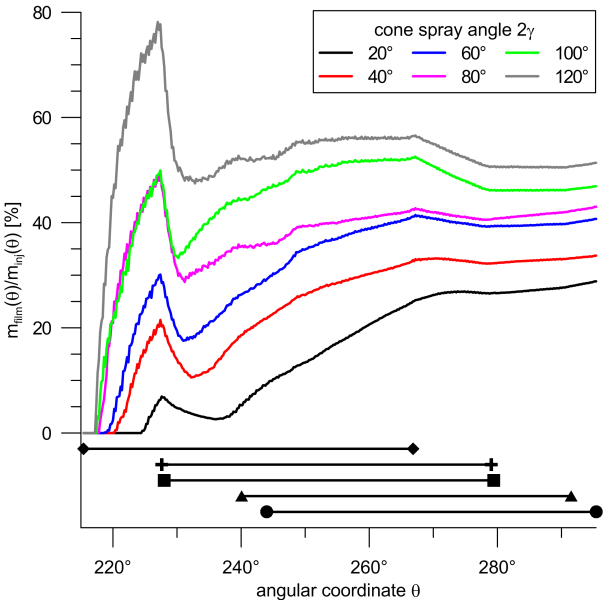

Figure 10: Effects of the cone spray angle on the liquid film formation

to volume ratio. The combined effect of these opposite phenomena is reported in Figure 11 at various injection pressures: from the overall heat transfer point of view, the impingement effect is remarkable at small cone angles ($2\gamma < 80°$) and overcomes the SMD one. The worst situation occurs at around 80° whereas the thermal power exchanged is minimized. Later on, the SMD effect tends to superimpose to the impingement one and leads to a slight increase of the thermal power exchanged even though the effective mass that performs this task is lower and lower, as demonstrated by Figure 10. Due to the tightness of the gap between stator and rotor along the axial length of the compressor, cone angles higher than 40° may reduce the cooling capabilities of the sprays up to 60 %. This decrease is mitigated increasing the injection pressure. Hence, despite strong assumptions were made on the two-dimensional nature of the spray and the absence of coalescence (enhanced in narrow sprays), small cone nozzles (γ around 15°) should be adopted to maximize the heat transfer capabilities of the spray in terms of residence time of the oil as droplets.

5. CONCLUSIONS

The current work investigated the energy saving potential of oil spray injections in sliding vane rotary compressors through the enhancement of the heat transfer between oil and air to approach an isothermal compression. A theoretical model of the innovative injection technique was developed. Based on a Lagrangian form of the conservation equations, the model follows the interactions between oil droplets and air from the spray breakup until the impingement on the metallic surfaces of the compressor cells. The effects of multiple injections can be superimposed to increase the cooling effects. The model was further validated

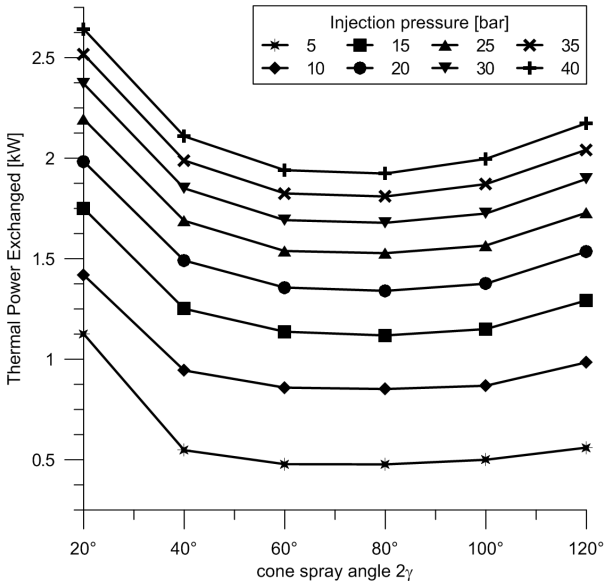

Figure 11: Effects of the cone spray angle on the thermal power exchanged

through an experimental activity on a mid-size SVRC. The compressor was equipped with a series of pressure swirl nozzles that sprayed the oil pressurized at 20 bar by a gear pump. Thanks to the enhanced heat transfer, a decrease on the mechanical power absorbed of 7.3 % was experimentally noticed. Despite the assumptions made, the overall model agreement with the experimental pressure trace retrieved from piezoelectric pressure transducers mounted on the compressor is satisfactory: the cell pressure at the injection end is matched until the discharge takes place. Furthermore, the spray evolution respects the experimental trends available in literature. In order to find an optimal set for the operating parameters of the injection, a parametric analysis was eventually carried out focusing on the oil pressure and temperature at the injection and the nozzle cone spray angle. Although high pressures lead to finer sprays, an asymptotic trend was noticed: over 20 bar the benefit on the overall thermal power exchanged (air cooling) is not convenient anymore. Moreover, at injection pressures higher than the line value, an auxiliary device is needed to pressurize the oil and the net specific benefit decreases. On the other hand, cold injections could be performed to enhance the cooling more than 30 % increasing the temperature difference between oil and air. To maximize the residence time of the droplets inside the compressor vanes, nozzles with narrow cone angles around 30° should be employed with axial injections. When considering variable speed drive compressors, the influence of the revolution speed on the optimal cone spray angle could be taken into account to evaluate the effects of a different centrifugal force on the droplets deviation towards the stator.

Acknowledgement

The work has been done under the FP7 Project "Complete Vehicle Energy-Saving CONVENIENT" founded by the European Commission.

REFERENCES

Abramzon, B., Sazhin, S., 2006. Convective vaporization of a fuel droplet with thermal radiation absorption. Fuel 85, 32 – 46. doi:10.1016/j.fuel.2005.02.027.

Aggarwal, S.K., Peng, F., 1995. A review of droplet dynamics and vaporization modeling for engineering calculations. Journal of Engineering for Gas Turbines and Power 117, 453–461. doi:10.1115/1.2814117.

Bianchi, G., Cipollone, R., in pressa. Friction power modeling and measurements in sliding vane rotary compressors. Applied Thermal Engineering .

Bianchi, G., Cipollone, R., in pressb. Theoretical modeling and experimental investigations for the improvement of the mechanical efficiency in sliding vane rotary compressors. Applied Energy .

Chen, J.L., Chen, G., Wells, M., 1993. Dynamic and static flow analysis of a gasoline fuel injector. Journal of Engineering for Gas Turbines and Power 115, 750–755. doi:10.1115/1.2906770.

Cipollone, R., 2014. Sliding vane rotary compressor technology and energy saving. Proceedings of the Institution of Mechanical Engineers, Part E: Journal of Process Mechanical Engineering doi:10.1177/0954408914546146.

Cipollone, R., Bianchi, G., Contaldi, G., 2012. Sliding vane rotary compressor energy optimization, in: ASME 2012 International Mechanical Engineering Congress and Exposition, American Society of Mechanical Engineers. pp. 69–80.

Cipollone, R., Valenti, G., Bianchi, G., Murgia, S., Contaldi, G., Calvi, T., 2014. Energy saving in sliding vane rotary compressors using pressure swirl oil atomizers. Proceedings of the Institution of Mechanical Engineers, Part E: Journal of Process Mechanical Engineering doi:10.1177/0954408914550356.

Cipollone, R., Valenti, G., Bianchi, G.e.a., 2013. Energy saving in sliding vane rotary compressors, in: Proceedings of 8th International Conference on Compressors and their Systems, Institution of Mechanical Engineers. pp. 173–182.

Cipollone, R., Vittorini, D., 2014. Energy saving potential in existing compressors, in: Proceedings of the 22nd International Compressor Engineering Conference, Purdue University.

C.N. Brown, N.L., 1991. A numerical study of fuel evaporation and transportation in the intake manifold of a port-injected spark-ignition engine. Journal of Automobile Engineering 205, 161–175.

Conde, M.R., 1996. Estimation of thermophysical properties of lubricating oils and their solutions with refrigerants: An appraisal of existing methods. Applied Thermal Engineering 16, 51 – 61. doi:10.1016/1359-4311(95)00011-2.

Ferreira, C.I., Zamfirescu, C., Zaytsev, D., 2006. Twin screw oil-free wet compressor for compressionabsorption cycle. International Journal of Refrigeration 29, 556 – 565. doi:10.1016/j.ijrefrig.2005.10.006.

Fujiwara, M., Osada, Y., 1995. Performance analysis of an oil-injected screw compressor and its application. International Journal of Refrigeration 18, 220 – 227. doi:10.1016/0140-7007(95)00008-Y.

Han, Z., Parrish, S., Farrell, P.V., Reitz, R.D., 1997. Modeling atomization processes of pressure-swirl hollow-cone fuel sprays. Atomization and Sprays 7, 663–684.

Laryea, G., No, S., 2004. Spray angle and breakup length of charge-injected electrostatic pressure-swirl nozzle. Journal of Electrostatics 60, 37 – 47. doi:10.1016/j.elstat.2003.11.001.

Liu, H., 1999. 4 - empirical and analytical correlations of droplet properties, in: Science and Engineering of Droplets. William Andrew Publishing, Norwich, NY, pp. 238 – 314. doi:10.1016/B978-081551436-7.50005-8.

Lottin, O., Guillemet, P., Lebreton, J.M., 2003. Effects of synthetic oil in a compression refrigeration system using r410a. part i: modelling of the whole system and analysis of its response to an increase in the amount of circulating oil. International Journal of Refrigeration 26, 772 – 782. doi:10.1016/S0140-7007(03)00064-1.

Mermond, Y., Feidt, M., Marvillet, C., 1999. Thermodynamic and physical properties of mixtures of refrigerants and oils. International Journal of Refrigeration 22, 569 – 579. doi:10.1016/S0140-7007(99)00015-8.

Paepe, M.D., Bogaert, W., Mertens, D., 2005. Cooling of oil injected screw compressors by oil atomisation. Applied Thermal Engineering 25, 2764 – 2779. doi:10.1016/j.applthermaleng.2005.02.003.

Radgen, P., 2001. Compressed air systems in the European Union: energy, emissions, savings potential and policy actions. LOG_X Verlag GmbH.

Seshaiah, N., Ghosh, S.K., Sahoo, R., Sarangi, S.K., 2007. Mathematical modeling of the working cycle of oil injected rotary twin screw compressor. Applied Thermal Engineering 27, 145 – 155. doi:10.1016/j.applthermaleng.2006.05.007.

Seshaiah, N., Sahoo, R., Sarangi, S., 2010. Theoretical and experimental studies on oil injected twin-screw air compressor when compressing different light and heavy gases. Applied Thermal Engineering 30, 327 – 339. doi:10.1016/j.applthermaleng.2009.09.010.

Spalding, D.B., 1953. The combustion of liquid fuels, in: Symposium (international) on combustion, Elsevier. pp. 847–864.

Stosic, N., Kovacevic, A., Hanjalic, K., Milutinovic, L., 1988. Mathematical modelling of the oil influence upon the working cycle of screw compressors, in: Proceedings of the International Compressor Engineering Conference, Purdue University.

Stosic, N., Milutinovi, L., Hanjali, K., Kovaevi, A., 1992. Investigation of the influence of oil injection upon the screw compressor working process. International Journal of Refrigeration 15, 206 – 220. doi:10.1016/0140-7007(92)90051-U.

US Department of Energy, 2003. Improving Compressed Air System Performance: a sourcebook for industry.

Valenti, G., Colombo, L., Murgia, S., Lucchini, A., Sampietro, A., Capoferri, A., Araneo, L., 2013. Thermal effect of lubricating oil in positive-displacement air compressors. Applied Thermal Engineering 51, 1055 – 1066. doi:10.1016/j.applthermaleng.2012.10.040.

Vittorini, D., Bianchi, G., Cipollone, R., in press. Energy saving potential in existing volumetric rotary compressors, in: Proceedings of the 69th Conference of the Italian Thermal Machines Engineering Association, Energy Procedia.